1   A Cadaveric Study Validating *in vitro* Monitoring Techniques to Measure the Failure

2   Mechanism of Glenoid Implants against Clinical CT

3

4   Sarah Junaid[1]*, Thomas Gregory[2,5], Shirley Fetherston[3], Roger Emery[4], Andrew A Amis[4,5],

5   Ulrich Hansen[5].

6

7   1. Mechanical Engineering and Design, Aston University, Birmingham, B4 7ET, UK

8   2. Service de Chirurgie Orthopedique et Traumatologique, Université Paris Descartes,

9   Hôpital Européen Georges Pompidou, France.

10   3. Radiology, St Mary's Hospital, London, United Kingdom

11   4. Musculoskeletal Surgery, Imperial College London, London, W6 8RF, UK.

12   5. Department of Mechanical Engineering, Imperial College London, SW7 2AZ, UK.

13

14   * Corresponding author: Sarah Junaid

15   Mechanical Engineering and Design

16   Aston University

17   Aston

18   Birmingham, B4 7ET, UK

19   Telephone: +44 (0)121 204 4177

20   Email: s.junaid@aston.ac.uk

21

22   **Author contributions statement:**

23   **Sarah Junaid:** Primary contribution to research design, the acquisition, analysis and

24   interpretation of data, drafting and revising the paper

25   **Thomas Gregory:** substantial contributions to the acquisition and interpretation of data and

26   editing the paper

27   **Shirley Fetherston:** substantial contributions to the acquisition and analysis of the data

28   **Roger Emery:** substantial contributions to research design and interpretation of data

29   **Andrew Amis:** substantial contributions to interpretation of data and editing the paper

30   **Ulrich Hansen:** substantial contributions to research design, analysis and interpretation of

31   data and editing the paper

32

33 **Abstract**

34 Definite glenoid implant loosening is identifiable on radiographs, however, identifying early

35 loosening still eludes clinicians. Methods to monitor glenoid loosening *in vitro* have not been

36 validated to clinical imaging. This study investigates the correlation between *in vitro*

37 measures and CT images. Ten cadaveric scapulae were implanted with a pegged glenoid

38 implant and fatigue tested to failure. Each scapulae were cyclically loaded superiorly and CT

39 scanned every 20,000 cycles until failure to monitor progressive radiolucent lines. The

40 superior and inferior rim displacements were also measured. A finite element (FE) model of

41 one scapula was used to analyse the interfacial stresses at the implant/cement and

42 cement/bone. All ten implants failed inferiorly at the implant-cement interface, two also

43 failed at the cement-bone interface inferiorly, and three showed superior failure. Failure

44 occurred at of $80,966 \pm 53,729$ (mean $\pm$ SD) cycles. CT scans confirmed failure of the

45 fixation, and in most cases, was observed either before or with visual failure, indicating its

46 capacity to detect loosening earlier for earlier intervention if needed. Significant correlations

47 were found between both increasing inferior rim displacement (ASTM standard F2028-14),

48 increasing vertical head displacement and failure of the glenoid implant. The FE model

49 showed peak tensile stresses inferiorly and high compressive stresses superiorly,

50 corroborating experimental findings. Similar failure modes have been cited in clinical and *in*

51 *vitro* studies. *In vitro* monitoring methods correlated to failure progression in clinical CT

52 images.

53 **Clinical Significance:** The study highlights failure at the implant-cement interface and early

54 signs of failure are identifiable in CT images.

55

56 Keywords: glenoid loosening, fixation failure, CT, radiolucent lines

57 **Introduction**

58 A study investigating total shoulder arthroplasty outcomes (TSA) found loosening to be the

59 most common complication.[1, 2] This has been confirmed by other recent studies[3, 4] and

60 has accounted for up to 44 % of glenoid implant failures.[5] In clinical and cadaveric studies

61 on glenoid fixation, the absence of visual observation requires investigators to depend on the

62 presence of radiolucent lines in radiographs and clinical examination to judge the quality of

63 the implant fixation. Clinically the majority of radiolucent lines have been identified in the

64 inferior region of the implant, possibly indicating glenoid loosening and a mechanical

65 weakness inferiorly.[6-8] Radiographs are fairly accurate when identifying advanced stages

66 of loosening, which is defined by a visible shift of the implant or a radiolucent line

67 encompassing the entire implant fixation, commonly referred to as 'definitely loose'.[5]

68 However, early loosening stages are ambiguous in radiographs and impossible to define

69 accurately. Even when identifying definite loosening, a study on failed TSA found 85 % of

70 retrieved glenoid implants that were definitely loose were identified from the radiographs[9],

71 which indicates an under estimation of the loosening problem.

72

73 *In vitro* studies have attempted to quantify glenoid loosening by measuring the horizontal rim

74 displacement during superior-inferior cyclic rim loading of the glenoid implant.[10-12] These

75 fatigue studies, which use bone substitute foam to eliminate the effect of bone variability,

76 found a positive correlation between inferior rim displacement and number of cycles.

77 However, the disadvantage in using this quantitative method is that these studies were not

78 able to visualise failure progression of the embedded glenoid. Therefore it is difficult to link

79 any quantitative data to actual failure. This gap has been addressed in two *in vitro* 2D studies

80 correlating failure progression with both rim displacement and head displacement.[13, 14]

81 The latter study allowed direct observation of the implant fixation, and found a correlation

82 between inferior fixation failure and superior and inferior rim displacements.[14] The idea of

83 using head displacement to monitor failure progression was also introduced.

84

85 A significant drawback to these *in vitro* studies is that clinical measurement methods such as

86 radiographs were not used to correlate their quantitative findings. In response to this, a study

87 using implants embedded in bone substitute investigated CT imaging to monitor early stages

88 of fixation failure.[15] The study found a correlation between radiolucent lines in the final

89 CT images and implant-cement interface fixation failure from sectioning the specimens. The

90 main drawback was the use of bone substitute, which allowed the displacement correlation to

91 be identified but does not directly represent the human glenoid bone structure, which is

92 structurally heterogeneous, highly variable and therefore can have variable bone-cement

93 interfacial strengths.

94

95 *In vitro* testing of glenoid loosening has attempted to quantify or monitor fixation failure

96 through rim displacements, head displacements, and CT imaging. However, there is a lack of

97 clarity on how these measures correlate to actual failure or failure progression. Comparing

98 these findings to the clinical setting is also limited due to lack of cadaveric testing. This

99 cadaveric study aims to identify any correlations between *in vitro* monitoring methods and

100 clinical methods to measure glenoid prosthesis failure. .

101

102 **Materials & Methods**

103

104 Eleven fresh-frozen cadaveric scapulae were used, with ethics committee approval. One was

105 excluded due to very poor sclerotic bone. Another was defined as partially sclerotic, but this

106 was included in the study, resulting in a total of ten scapulae that were implanted and tested.

107

108 *Monitoring Methods*

109 Three methods were used to observe and monitor failure progression; quantitative *in vitro*

110 measures, qualitative *in vitro* observations and clinical observations. These will be referred to

111 as quantitative, qualitative and clinical for the rest of the paper. Quantitative measures used

112 were superior and inferior rim displacements as specified by the ASTM testing standard

113 (F2028-14[16]) and vertical head displacement changes. The qualitative measures used were

114 visual observation during testing and cross-sectional observation under microscopy post-

115 testing. Finally, the clinical measure used was radiolucent lines in CT images of the

116 specimens. Correlations were sought between the qualitative and quantitative measures and

117 the clinical observations.

118

119 *Specimen Preparation*

120 The ten scapulae were implanted with a commercially available glenoid implant, an Aequalis

121 all-polyethylene, curved-back, pegged design (Tornier Inc., Grenoble, France) (Figure 1).

122 Three small, six medium and one large glenoid with radial curvatures of 27.5 mm, 30 mm

123 and 32.5 mm respectively were implanted by an experienced shoulder surgeon (T.G.). The

124 soft tissue and labrum were excised. The glenoid surface was reamed, removing the cartilage

125 layer, and care was taken to maintain the subchondral layer. The glenoid implants were

126 cemented using Simplex® bone cement (Stryker Europe, Montreux, Switzerland). The

127 scapulae were cut to size using an Exakt 310 CP diamond-tipped high precision saw (Exakt

128 Technologies Inc., Oklahoma City, USA) and cemented using Simplex® bone cement into the

129 specimen holder. Care was taken to ensure the correct seating of the glenoid component with

130 no tilt (Figure 1). Two holes were drilled into each glenoid implant to accommodate a 2 mm

131 diameter rod at the superior and inferior edge of the glenoid, 2.5 mm from the corresponding

132   rim. The two rods were prepared as reference points to measure the corresponding rim

133   displacements via two displacement transducers (LVDTs) (Figure 2).

134

135   *Mechanical Test*

136   The scapulae were cemented into the specimen holder and tested using a testing rig compliant

137   to the ASTM standard F2808-14.[16] A compressive horizontal load of 750 N was applied

138   throughout. A 24 mm humeral head manufactured by the implant company was used to

139   articulate onto the implants for all specimens. Thus, the three glenoid sizes; small, medium

140   and large, corresponded to a radial mismatch of 3.5, 6 and 8.5 mm respectively. The

141   specimens were tested without a water bath at room temperature, and the scapulae and joints

142   were kept wet via a water spray. LVDTs were attached directly to the specimen and

143   horizontally aligned to measure horizontal rim displacement at the superior and inferior rim

144   via reference pins inserted at the implant rim edge as specified by the standard[16] (Figure 2).

145   The rim displacements were measured every 2000 cycles without stopping the test with the

146   inferior rim displacement as the primary outcome measure (ASTM F2028-14). Every 4000

147   cycles the vertical head displacement was readjusted to maintain the testing loads.

148

149   The loading regime was derived from the subluxation curves of two medium glenoid

150   prostheses implanted in bone substitute. The vertical load was chosen to be 400 N by deriving

151   90% of the subluxation load. A common load was used throughout, despite testing 3 different

152   implant sizes. The subluxation load differences between large and medium glenoid prostheses

153   were comparable at 500 N and 465 N respectively. Thus a standardised loading of 400 N was

154   used for all specimens.

155

156 ***CT Scans***

157 CT scans were taken of all the scapulae before implantation, after implantation, at 20,000,

158 40,000, 60,000 cycles and after failure or at 200 000 cycles if failure did not occur.

159

160 During testing, failure visually was defined in two stages (Figure 3), initial failure was

161 indicated by visible distraction of the inferior glenoid rim from the cement or bone substitute

162 block. Partial failure was defined as the point when the inferior pegs were visible during

163 inferior rim distraction, where the test was stopped. Partial failure is referred-to in the

164 following text as failure. Superior bone crushing was defined by visible embedding of the

165 superior implant rim or bone fracture and superior failure was defined as visible distraction of

166 the superior rim. "CT partial failure" was defined as a radiolucent line between the implant

167 rim and the cement and the bone or between the cement and bone (Figure 4). "Complete

168 failure" was defined as a radiolucent line reaching the inferior pegs in the CT images.

169 Microscopic images were compared to the final CT image.

170

171 ***Post-Testing Observations***

172 After testing to failure or to 200,000 cycles, the specimens were sectioned through the

173 superior-inferior centreline using an Exakt 310 CP diamond-tipped saw (Exakt Technologies

174 Inc., Oklahoma City, USA) and the fixation and bone conditions were observed under a

175 Nikon SMZ 800 microscope (Nikon Instruments Inc., New York, USA) with a magnification

176 of x20.

177 Statistical significance between the rim displacement measures and correlation to visual

178 failure as well as vertical head displacement to visual failure were tested using a single factor

179 ANOVA tests.

180

181 ***Finite Element Modelling***

182 A three-dimensional finite element (FE) model was constructed using a CT scan of one of the

183 scapulae. Amira® (Visage Imaging, California, USA) was used to construct the tetrahedral

184 mesh using over 100,000 elements and the glenoid implant model acquired from the implant

185 company (Tornier Inc., Grenoble, France) was inserted into the bone model. Marc/Mentat

186 2001 (MSC Software Corporation, California, USA) was used to perform the FE analysis.

187 The material properties of the bone were assigned using an in-house program.[17] The Carter

188 & Hayes (1977)[18] relation was used to describe the material properties of bone from the

189 CT number: $E=2875\rho_{app}^{3}$, where E is the Young's modulus, ρ_{app} is the apparent density and

190 CT numbers 30 to 2000 correspond to densities 0.3 to 1.8 g/cm^3 on a linear scale. The

191 strength of the cancellous bone was calculated using the following relationship: $S=51.58\rho^{2}$

192 using the lowest density value in the bone image of 0.3 g/cm^3 (Carter & Hayes 1977).[18]

193 PMMA Bone cement was given a Young's modulus of 2.2 GPa and Poisson's ratio of

194 0.3.[19]

195

196 The contact surfaces were bonded and the humeral head was modelled as a rigid hemisphere.

197 The scapula was cut to size, as in the in-vitro test. The surface nodes of the scapula beyond

198 the scapula neck were constrained in all 3 axes. The frictional coefficient between the

199 humeral head and glenoid was 0.07.[11] A compressive load of 750 N was applied to the

200 humeral head and a vertical load was applied via head displacement of 11 mm, to generate a

201 load/displacement subluxation curve. The FE mesh was tested to load convergence.

202

203 **Results**

204   *Qualitative Measurement Results*

205 All ten implants visibly failed except one, which only partially failed (Figure 3) where the

206 test stopped after 200,000 cycles. Six failed exclusively at the implant-cement interface, two

207 failed both at the implant-cement and cement-bone interface and two failed superiorly due to

208 cortical bone failure (Figure 4). Implant failure occurred between 16,300 and 122,500 cycles,

209 with a mean (± SD) of 80,966 ± 53,729 cycles. The earliest specimen to fail had previously

210 been identified as partially sclerotic. The partially failed implant was stopped at 200,000

211 cycles, although some superior and inferior implant-cement distraction was observed and CT

212 scans revealed initial good implant seating. All final CT scans confirmed failure, which were

213 observed visually (Figure 5), however, in three specimens it was difficult to identify which

214 interface loosening was apparent either visually or with CT. No significant difference was

215 found between the three radial mismatches with respect to cycles to failure.

216

217 The visual examination of the sectioned specimens confirmed clear failure at the implant-

218 cement interface and superior bone crushing, as was observed from inspection of unsectioned

219 specimens (Figure 6). The microscopic study revealed the cement thickness varied from 0.5-

220 1.5 mm and was cracked in three specimens at one of the peg junctions where bending

221 stresses had been experienced. There were no other apparent cement fractures anywhere else.

222 In one case, the implant completely detached at the implant-cement interface, the cement

223 embedded in the peg grooves was still intact.

224

225 *Quantitative Measurement Results*

226 Inferior rim displacement and vertical head displacement both increased with observed

227 failure (Figure 7). The positive correlation between vertical head displacement before failure

228   and at failure was statistically significant (p < 0.05). This was also true for the inferior rim

229   displacement (p < 0.05). The mean vertical head displacement (± SD) before and after failure

230   was 2.3 ± 1.1 mm and 3.5 ± 1.5 mm respectively.

231

232   ***Clinical Measurement Results***

233   All four failure measures: clinical CT, qualitative visual, quantitative vertical head and

234   quantitative inferior rim displacement, positively correlated with cycles to failure (Figure 8

235   and Table 1). On average, failure was identified in clinical CT images before visual failure

236   was observed (Figure 8). This observation was found in 8/10 shoulders. In the remaining two

237   shoulders, CT and visual failure were observed together in one and visual failure observed

238   first in the other.

239   Quantitatively, mean vertical head displacement increased with cycles to failure, visual

240   failure and CT failure in all ten specimens. On average inferior rim displacement did not

241   change at 33-44% cycles to failure (partial failure stage) until 100% failure occurred.

242   Furthermore, the inferior rim displacement fluctuated throughout testing compared to vertical

243   head displacement, which progressively increased.

244

245   ***Finite Element Modelling***

246   The implant/cement interface normal stress predicted by the FE model showed superior

247   compressive stresses and inferior tensile stresses. Tensile peak stresses were found at the base

248   of the pegs (2.5 MPa) and peaked at the inferior edge of the implant (1 MPa).

249

250

251   The strength of the cancellous bone was calculated using the lowest bone density as 4.6 MPa,

252   the compressive stresses in the bone exceeded this superiorly during loading, corroborating

253   the experimental finding of superior bone crushing (Figure 10).

254

255   **Discussion**

256   The most important finding of this study was the significant correlations found between three

257   laboratory-based qualitative and quantitative measures of glenoid loosening (visual failure,

258   inferior rim displacement and vertical head displacement) and clinical CT images of

259   loosening. Using the ASTM F2028-14[16] testing method allowed a standardised and

260   repeatable method of mechanically testing the integrity of the glenoid prosthesis/cement/bone

261   interface. For this study, the standard was used to test glenoid fixations in cadaveric bone

262   rather than bone substitute. The advantage of quantifying failure is that it serves as a

263   comparative measure between implant designs and allows for controlled testing of various

264   surgical conditions such as poor bone quality, cement interdigitation and bone wetness. From

265   the three measurements used in this study visual failure was the surest way of identifying

266   failure, however, it is subjective and labour intensive. Inferior rim displacement is not

267   subjective but requires alteration of the implant by drilling or fixing a measuring platform to

268   the rim. Finally the head displacement does not require any alterations to the test or additional

269   measuring equipment, however, requires load-controlled testing. All three measures had

270   previously not been directly compared to what is observed clinically using cadaveric bone.

271   This study has shown that what may be seen in clinical CT imaging correlated with detailed

272   measurements of loosening phenomena on the specimens.

273

274   Although the sample size was small, all ten cadaveric scapulae teste failed inferiorly at the

275   implant-cement interface, and two of these also failed at the cement-bone interface. No

276   specimen failed at the cement-bone interface alone, however superior bone crushing was also

277   observed clearly in three specimens. The CT scans indicated failure at the observed interface

278   in seven cases and was able to detect failure before or with visual failure in nine specimens.

279   All *in vitro* measurements correlated with CT failure, with quantitative rim displacement and

280   head displacement both showing a significant increase from no failure to failure ($p < 0.05$)

281   (Figure 7). The FE model showed peak tensile loads at the inferior rim and at the base of the

282   inferior pegs. Unpublished work in our laboratory have found implant/cement interface

283   strengths at between 0 and 1 MPa for smooth implant surfaces, placing the peak tensile

284   stresses within the failure range, thus possibly corroborating the experimental findings

285   (Figure 9).

286   Furthermore, the 4.6 MPa predicted bone failure compressive strength was exceeded during

287   the tests. This prediction was corroborated by the superior crushing found in seven of the ten

288   experimental samples.

289

290   Clinical results have indicated predominantly cement-bone failure via radiographic

291   examination. This study has investigated this phenomenon using a standardised *in vitro* cyclic

292   test, post-testing microscopic evaluation and monitoring failure both visually and

293   quantitatively. The question of where the fixation is weakest is not a simple one, considering

294   implant roughness, cement interdigitation, cement thickness, wetness of the bone and bone

295   quality all contribute to the interfacial conditions. Using a smooth implant in this case has

296   demonstrated that the fixation is weakest at the implant-cement interface. The FE model

297   indicated stresses exceeding the strength of a smooth implant-cement interface.

298

299   Clinical studies have similarly shown loosening at the inferior part of the fixation [6-8]. One

300   study by Nyffeler et al. 2003[20] found a retrieved loosened glenoid had clearly failed at the

301   implant-cement interface, however, most studies (with few retrieved glenoids) indicate failure

302   at the cement-bone interface. The question is why isn't the implant-cement interface observed

303   as loosening clinically?

304

305   Although the causes of failure were primarily found at the implant-cement interface

306   inferiorly, the problem of bone compression, found in a third of the specimens in this study,

307   will also have a long-term effect on bone remodelling. One of the drawbacks in this testing

308   method is that the mechanobiological element is completely eliminated from the fatigue test.

309   The results in this study suggest that improving the mechanical fixation of the glenoid

310   implant at the implant-cement interface may improve the short to mid-term outcomes of the

311   implant. However, the biological effects will inevitably be one of the primary concerns in

312   long-term outcomes of the fixation. It is at this point that the cement-bone interface, initially

313   an excellent mechanical interlocking mechanism, may biologically break down into a

314   fibrocartilage-cement interface. This fibrocartilage layer may be the cause of the progressive

315   radiolucent lines found in radiographs [21]. It is therefore understandable that early static

316   images of the shoulder do not reveal gaps in the implant-cement interface, which would

317   manifest under dynamic movement. In a recent radiographic study, Fox et al. (2013)

318   highlighted late radiographic failure occurring after 5 years and called for the need for design

319   innovations to improve glenoid fixations.[3] The study also highlighted glenoid implants "at

320   risk" of radiographic failure were linked with superior subluxation of the humeral head,

321   which may indicate the problem of high vertical head displacement, a measure used in this

322   paper. This is further supported by a fluoroscopic study showing higher superior humeral

323   head migration under dynamic movement compared to static, indicating an underestimation

324   of true head migration during movement.[22] These findings are possibly supported by an

325   earlier multicentre study in 2002 that among the complications, five shoulders suffered from

326 postoperative humeral head subluxation/dislocation, from which three were due to glenoid

327 loosening and one due to poor rotator cuff support.[23]

328

329 Partial implant embedding superiorly was observed in six cases during testing, however, the

330 cross-sections did not reveal obvious bone crushing in all of them. Despite this, embedding

331 affects the subluxation mechanics, possibly exaggerating further the 'rocking horse effect'.

332 Thus, if the implant can avoid embedding into the bone the stability and longevity of the

333 fixation will improve. It may simply be a question of implant seating and correct sizing of the

334 implant to align the implant rim with the cortical glenoid rim as also suggested by Iannotti et

335 al. 2005.[24] Maintaining the subchondral plate is also important to maintain good glenoid

336 seating. However, this study shows radial mismatch does not appear to be critical, which is

337 supported by previous cadaveric and clinical studies.[25, 26]

338

339 There are several drawbacks in this study; firstly, the rim displacements were often difficult

340 to monitor, due to the compliance of the implant polymer. A stronger correlation to CT and

341 visual failure was found when monitoring failure using vertical head displacement compared

342 to inferior rim displacement. Unfortunately due to the relatively few CT data points for each

343 specimen, it was not possible to identify whether the changes in displacements were directly

344 a result of or preceding failure. More CT scans would be necessary for this analysis. Vertical

345 head displacement best matched visual failure, although this match was not as close as

346 expected. Interestingly, the increased vertical head displacement preceded visual failure in

347 some cases. This supports the "rocking horse" effect explanation, where increasing head

348 translation leads to fixation failure.

349

350   The loading regime was displacement controlled and was adjusted every 4000 cycles to

351   maintain consistent loads throughout the tests. Although this would have impacted on the

352   number of cycles to failure, it was necessary to ensure the progression of failure was

353   captured. If tested under load control there was a greater risk that the stages of failure would

354   not be captured, which was an important objective in the study. Despite this limitation, the

355   outcomes on cycles to failure were not intended as directly equivalent to clinical failure and

356   therefore was not set up to test how long the fixation would last clinically.

357

358   The third drawback is that only one implant design was tested, thus comments regarding

359   design weaknesses and stress raisers are limited to the particular design. However, restricting

360   the test to one design allowed observations on generic parameters to be made such as the

361   apparent weakness of the implant-cement strength using a smooth implant. Although using a

362   smooth implant inevitably weakened the interface, this worst-case scenario is useful to

363   analyse and the most clinically relevant as all companies, with one exception, do not roughen

364   the glenoid implant for cemented TSA.

365

366

367   The finite element analysis used to evaluate the stress/strain behaviour was limited to one

368   specimen. Although this limits the discussion on the internal loading behaviour, all specimens

369   demonstrated similar failure modes and the FE analysis did corroborate the experimental

370   findings of inferior tensile stresses and implant embedding superiorly in the shoulder.

371   Therefore the similarity in failure behaviours between samples gives some weight to the FE

372   analysis being representative of the general loading trend. However a more detailed

373   investigation on the minor distinctions between samples from experimental observations may

374   still benefit from individual FE analysis.

375

376 Finally, a cadaveric study of 10 scapulae is a small one. Variability in bone quality, properties

377 and various implant sizes, resulting in variable radial mismatches, makes conclusive remarks

378 more difficult. In addition, clinical loosening may be affected by biological processes over

379 time, which do not occur with cadaveric tests.. This has meant the results in the study may

380 not hold the power needed to conclusively state the strength of using CT images for

381 measuring loosening progression. A post-hoc power analysis indicates over 70 % power

382 (α=0.05). However it does corroborate the glenoid implant bone substitute study that showed

383 a link between interface failure using CT images and actual failure after cutting the

384 samples.[15] The outcomes also highlight a possible alternative to radiographs that is more

385 informative than other methods on the state of the glenoid interface. Furthermore the positive

386 correlation between quantitative measures and failure were found to be consistent in all

387 samples and also corroborated previous studies.[13, 14] Despite these limitations, testing the

388 cadavers to failure *in vitro* has allowed valuable insight into the mechanics of the cemented

389 fixation and the various parameters that contribute to the failure of the fixation.

390

391 Most clinical studies use radiographs, a common practice to assess the extent of loosening.

392 However, CT has been shown to be better at predicting loosening.[8] Aliabadi et al.

393 (1988)[27] found no correlation between radiolucent lines around the glenoid in radiographs

394 and pain, function and range of motion. Similarly Yian et al. (2005)[8] found no correlation

395 between radiolucent lines observed on plane radiographs and pain, however, a correlation

396 was found between radiolucent lines observed in CT and pain. Likewise, Nagels et al.

397 (2002)[7] found, using RSA techniques to monitor glenoid motion and loosening, that RSA

398 was better at detecting glenoid loosening compared to radiographs. The non-specificity of

399 radiolucent lines in detecting loosening and joint function is discussed further by Kovacevic

400 et al. 2014.[28] Thus, although radiographs have been useful to analyse grossly loose

401 implants, monitoring early signs of failure is hit and miss. Gregory et al. 2009 further

402 demonstrated the superiority of CT over radiographs, showing CT failure correlating to

403 observed failure of glenoid implants in bone substitute. This paper reports on the first

404 cadaveric study to show a correlation between actual failure progression *in vitro* to failure

405 observed on CT images and further correlates the *in vitro* quantitative measures to CT failure.

406

407 The issue of substantial radiation dose from CT scans compared to radiographs and

408 subsequently patient safety is a concern. Therefore using CT imaging in its current form may

409 be more suited for more critical cases. However, there is ongoing research and discussion on

410 optimising CT parameters to minimise dosage and achieve the required image accuracy.[29]

411 There may be some way to go to find a practical solution to the problem of detecting implant

412 loosening clinically. Despite this the outcomes of this study sheds some light into

413 understanding mechanical loosening. Furthermore the use of CT scanning for implant testing

414 and design development is useful and a more clinically relevant measure of loosening.

415

416 **Conclusion**

417 Inferior rim displacement and vertical head displacement were both shown to correlate to

418 progressive failure *in vitro*. Monitoring rim displacement is technically more difficult to

419 implement, highlighting the shortcomings of using this method. Vertical head displacement

420 overcomes this problem. Both measures were found to correlate to visualisation of interface

421 failure in CT scans, highlighting the possible usefulness of assessing failure from CT images

422 in clinical practice.

423

424   Comparative study of various glenoid designs will require a large sample size, which is

425   unobtainable in a cadaveric study. For such a study the use of a bone substitute with reliable

426   properties is desirable. This study will therefore be an important validation step for

427   investigating design parameters in commercial implants using bone substitute foam as the

428   substrate.

429

430   **Acknowledgements**

434

435 **References**

436 1.   Bohsali K, Wirth M, Rockwood Jr C. 2006. Complications in Total Shoulder

437   Arthroplasty. *J Bone Joint Surg Am* **88**:2279-92.

438 2.   Wirth M, Rockwood Jr C. 1996. Current Concepts Review - Complications of Total

439   Shoulder-Replacement Arthroplasty. *J Bone Joint Surg Am* **78**:603-16.

440 3.   Fox T, Foruria A, Klika B, et al. 2013. Radiographic Survival in Total Shoulder

441   Arthroplasty. *J Shoulder Elbow Surg* **22**:1221-7.

442 4.   McLendon P, Schoch B, Sperling J, et al. 2017. Survival of the Pegged Glenoid

443   Component in Shoulder Arthroplasty: Part Ii. *J Shoulder Elbow Surg* **26**:1469-76.

444 5.   Torchia M, Cofield R, Settergren C. 1997. Total Shoulder Arthroplasty with the Neer

445   Prosthesis: Long-Term Results. *J Shoulder Elbow Surg* **6**:495-505.

446 6.   Klepps S, Chiang A, Miller S, et al. 2005. Incidence of Early Radiolucent Glenoid

447   Lines in Patients Having Total Shoulder Replacements. *Clin Orthop Relat Res*

448   **435**:118-25.

449 7.   Nagels J, Valstar E, Stokdijk M, et al. 2003. Patterns of Glenoid Component

450   Loosening. *J Bone Joint Surg Br* **85-B**:79.

451 8.   Yian E, Werner C, Nyffeler R, et al. 2005. Radiographic and Computed Tomography

452   Analysis of Cemented Pegged Polyethylene Glenoid Components in Total Shoulder

453   Replacement. *J Bone Joint Surg Am* **87**:1928-36.

454   9.   Franta A, Lenters T, Mounce D, et al. 2007. The Complex Characteristics of 282

455   Unsatisfactory Shoulder Arthroplasties. *J Shoulder Elbow Surg* **16**:555-62.

456   10.   Anglin C. Shoulder Prosthesis Testing: Queen's University, Kingston; 1999.

457   11.   Anglin C, Wyss U, Pichora D. 2000. Mechanical Testing of Shoulder Prostheses and

458   Recommendations for Glenoid Design. *J Shoulder Elbow Surg* **9**:323-31.

459   12.   Oosterom R, Rozing P, Verdonschot N, et al. 2004. Effect of Joint Conformity on

460   Glenoid Component Fixation in Total Shoulder Arthroplasty. *Proc Inst Mech Eng H*

461   **218**:339-47.

462   13.   Junaid S, Gupta S, Sanghavi S, et al. 2010. Failure Mechanism of the All-

463   Polyethylene Glenoid Implant. *J Biomech* **43**:714-9.

464   14.   Junaid S, Sanghavi S, Anglin C, et al. 2017. Treatment of the Fixation Surface

465   Improves Glenoid Prosthesis Longevity in-Vitro. *J Biomech* **61**:81-7.

466   15.   Gregory T, Hansen U, Taillieu F, et al. 2009. Glenoid Loosening after Total Shoulder

467   Arthroplasty: An in Vitro Ct-Scan Study. *J Orthop Res* **27**:1589-95.

468   16.   F2028-14 A. Standard Test Methods for the Dynamic Evaluation of Glenoid

469   Loosening or Disassociation. West Conhohocken, PA: ASTM International; 2014.

470   17.   Hopkins A. Biomesh-F (Version 1_W) [Software]. 2008.

471   18.   Carter D, Hayes W. 1977. The Compressive Behavior of Bone as a Two-Phase Porous

472   Structure. *J Bone Joint Surg Am* **59**:954-62.

473   19.   Lewis G. 1997. Properties of Acrylic Bone Cement: State of the Art Review. *J*

474   *Biomed Mater Res A* **38**:155-82.

475   20.   Nyffeler R, Anglin C, Sheikh R, et al. 2003. Influence of Peg Design and Cement

476   Mantle Thickness on Pull-out Strength of Glenoid Component Pegs. *J Bone Joint*

477   *Surg Br* **85**:748-52.

478   21.   Wirth M, Korvick D, Basamania C, et al. 2001. Radiologic, Mechanical, and

479   Histologic Evaluation of 2 Glenoid Prosthesis Designs in a Canine Model. *J Shoulder*

480   *Elbow Surg* **10**:140-8.

481   22.   Teyhen D, Christ T, Ballas E, et al. 2010. Digital Flouroscopic Video Assessment of

482   Glenohumeral Migration: Static Vs. Dynamic Conditions. *J Biomech* **43**:1380-5.

483   23.   Norris T, Iannotti J. 2002. Functional Outcome after Shoulder Arthroplasty for

484   Primary Osteoarthritis: A Multicenter Study. *J Shoulder Elbow Surg* **11**:130-5.

485   24.   Iannotti J, Spencer Jr E, Winter U, et al. 2005. Prosthetic Positioning in Total

486   Shoulder Arthroplasty. *J Shoulder Elbow Surg* **14**:S111-S21.

487   25.   Karduna A, Williams G, Williams J, et al. 1997. Joint Stability after Total Shoulder

488   Arthroplasty in a Cadaver Model. *J Shoulder Elbow Surg* **6**:506-11.

489   26.   Young A, Walch G, Boileau P, et al. 2011. A Multicentre Study of the Long-Term

490   Results of Using a Flat-Back Polyethylene Glenoid Component in Shoulder

491   Replacement for Primary Osteoarthritis. *J Bone Joint Surgery Br* **93-B**:210-6.

492   27.   Aliabadi P, Weissman B, Thornhill T, et al. 1988. Evaluation of a Nonconstrained

493   Total Shoulder Prosthesis. *Am J Roentgenol* **151**:1169-72.

494   28.   Kovacevic D, Hodgins J, Bigliani L. 2014. Lucent Lines and Glenoid Components:

495   What Do They Portend? *Semin Arthroplasty* **25**:277-85.

496   29.   Lalone E, Fox A, Kedgley A, et al. 2011. The Effect of Ct Dose on Glenohumeral

497   Joint Congruency Measurements Using 3d Reconstructed Patient-Specific Bone

498   Models. *Physics in Medicine & Biology* **56**:6615.

499

500

Figure 1. Curved-back cemented glenoid implant (left). Cadaveric scapula cemented and potted for testing (right).
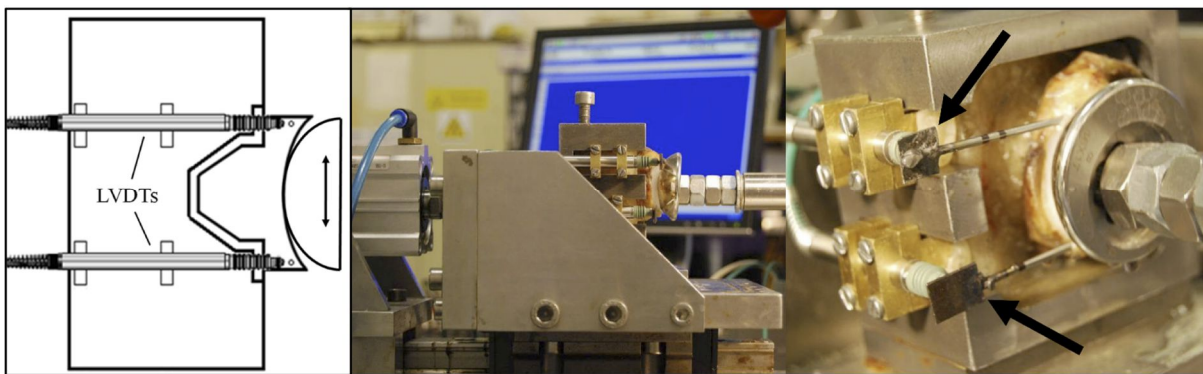
Figure 2. Mechanical glenoid fixation loosening cadaveric test (left). Reference pins (arrows) were used to monitor horizontal rim displacement using LVDTs attached directly to the specimens (right).

512 **Figure 3.** Failure definition: "partial failure" as inferior rim distracts away from cement (left)
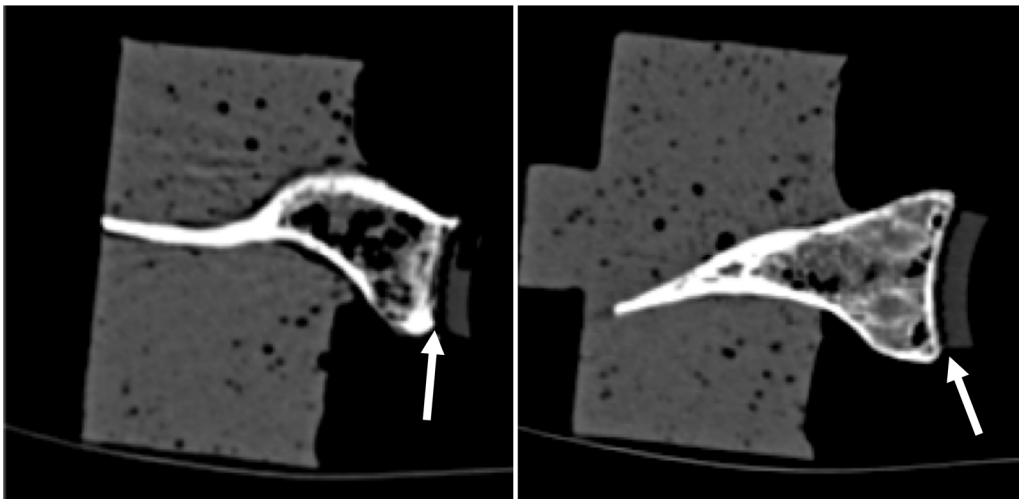
513 and "failure" as inferior pegs visible (right).

514

515

516 **Figure 4.** Superior failure-rim distracts away from cement (left) and bone crushing-bone

517 fracture or implant embedding (right).

518

519

520 **Figure 5.** CT slices of the transverse plane showing an example of superior (left) and inferior
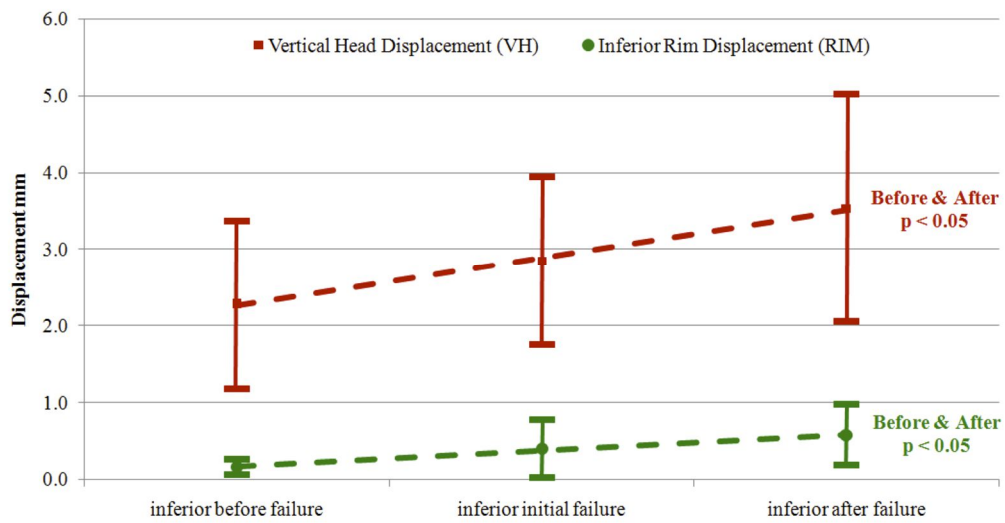
521 (right) failure at the implant-cement interface in a specimen.

522
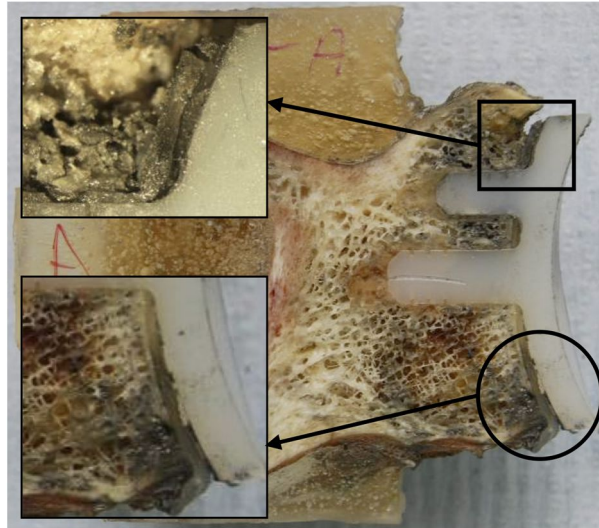
523

524   **Figure 6.** Cross-sectional slice of same specimen as CT after failure. Note: inferior failure of

525   the implant-cement (circle) and superior bone crushing (square).
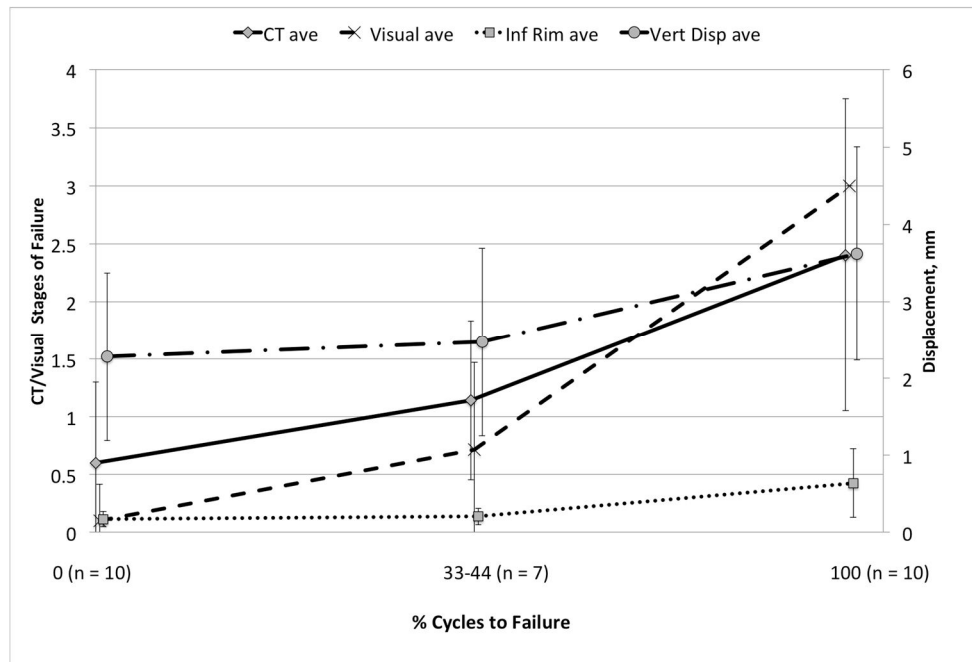
526

527

528   **Figure 7.** Positive correlation between vertical head displacement ($p < 0.05$) and inferior rim

529   displacement ($p < 0.05$) with visual failure.

530

531

Figure 8. A plot of the mean clinical CT failure* and qualitative visual measures* with quantitative inferior rim and vertical head displacement against cycles to failure, normalised to a percentage. The plot shows correlation between displacements with CT and visual failure. * No failure = 1, partial failure = 2 and failure = 3.
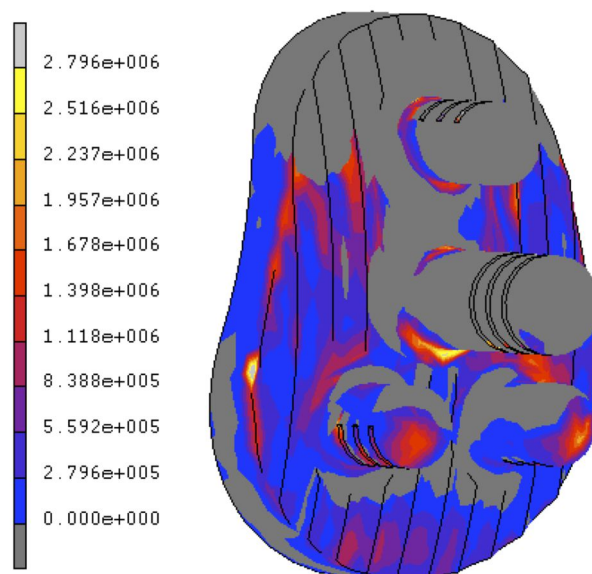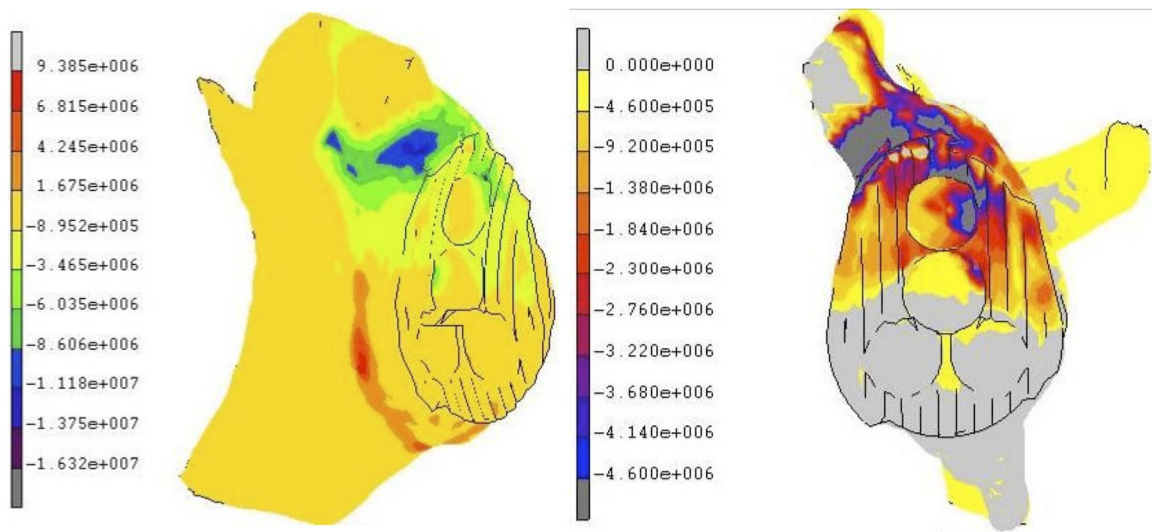

Figure 9. Tensile normal contact stresses at the implant/cement interface. Note: peak stresses at the inferior edge and pegs reaching up to 1 and 2.5 MPa respectively.

541

542

543 **Figure 10.** Color plot of the cadaveric bone showing minimum principal stress (compressive

544   stresses-blue) and maximum principal stress (tensile stresses-red) (left). Color plot of

545   minimal principal stress (compressive only) showing dark grey areas exceeding 4.6

546   MPa (predicted bone strength) (right).

547

548

549 **Table 1.** Tabulated form of figure 7 showing comparison of percentage cycles to failure at no

550 failure (0%), partial failure (33-44%) and failure (100%) compared to the four failure

551 measures; clinical CT failure, qualitative visual failure, quantitative inferior rim

552 displacement and quantitative vertical head displacement respectively. * No failure =

553 1, partial failure = 2 and failure = 3. ** Three implants failed before partial failure

554 was captured.

% Cycles to Failure	CT Failure*		Visual Failure*		Inferior Rim Displacement (mm)		Vertical Head Displacement (mm)	
	Mean	SD	Mean	SD	Mean	SD	Mean	SD
0% (n=10)	0.6	0.7	0.1	0.3	0.2	0.1	2.3	1.1
33-44% (n=7)**	1.1	0.7	0.7	0.8	0.2	0.1	2.5	1.2
100% (n=10)	2.4	1.3	3.0	0.0	0.6	0.4	3.6	1.4